Luiz Alberto Lisboa da Silva Cardoso, Miguel Comesaña Martinez,
Andrés Augusto Nogueiras Meléndez, João Luiz Afonso

“Dynamic Inductive Power Transfer Lane Design for E-Bikes”

IEEE 19th International Conference on Intelligent Transportation Systems (ITSC), pp. 2307-2312,

Rio de Janeiro, Brazil, Nov. 2016.

https://ieeexplore.ieee.org/document/7795928

DOI: 10.1109/ITSC.2016.7795928

ISBN: 978-1-5090-1889-5

L. A. L. Cardoso, M. C. Martinez, A. A. N. Melendez, J. L. Afonso, "Dynamic inductive power transfer lane design for e-bikes," in IEEE 19th International Conference on Intelligent Transportation Systems (ITSC), 2016, pp. 2307–2312. DOI 10.1109/ITSC.2016.7795928
ISBN 978-1-5090-1889-5016

Dynamic Inductive Power Transfer Lane Design for E-Bikes*

L. A. Lisboa Cardoso, *Member, IEEE*, M. Comesaña Martinez, *Student Member, IEEE,*
A. A. Nogueiras Meléndez, *Senior Member, IEEE*, and João L. Afonso, *Senior Member, IEEE*

***Abstract*— This paper presents the concept and initial test results of an inductive lane design capable of dynamic and wirelessly transfer power to electric bicycles (e-bikes). On the lane side, a sequence of oblong primary coils embedded underneath ground surface, along the vehicle path, can be independently excited by high frequency alternating current. The oscillating magnetic field of each primary coil is individually enabled when a Radio Frequency Identification (RFID) tag on board of the e-bike is detected and authenticated by an auxiliary coil laying close to that primary coil. On the e-bike, energy for the powertrain is harvested from the lane by a secondary coil that is installed around its rear wheel. When the e-bike is moving over inter-coil gaps, or anywhere away from the inductive lane, on-board power is sustained with the excess energy stored during transits over energized coils. Preliminary results from a prototyped module demonstrate the feasibility of the system, which could also be used by similarly adapted lightweight electric vehicles, such as rickshaws, electric wheel chairs and other electric personal mobility devices, favoring a new, low cost, sustainable urban modal variant.**

I. Introduction

Electric mobility has been considered a cleaner alternative to thermal engine based vehicles that use fossil fuels since their quasi-simultaneous introduction in the late 19th century. Initial market acceptance of electric vehicles (EV) was such that in 1900, 38% of all automobiles sold in the United States were powered by electricity, while only 22% by gasoline [1]. The electrics, however, virtually disappeared shortly after, for economical and technical reasons, leaving the cities overcrowded with the pollutant gasoline and, from the 1930s on, diesel engine vehicles.

One dominating technical reason was the driving range limitation resulted from the low energy density of early lead-acid type batteries, which were based on Gaston Planté's 1859 design. Another important reason was the relatively high complexity and cost of recharging stations (formerly based on rotary converters and then on mercury arc rectifiers), if compared to the practicality of liquid gasoline refueling stations.

Along the last two decades, modern brushless electric motors and advanced solid state power electronics came into scene together with higher capacity lithium batteries, and a profusion of new EV designs regained market attention, with current predictions indicating that the use of this technology will continuously grow until the fossil fuel engines become obsolete for most urban transportation applications. But while modern batteries do provide a much better performance, in terms of energy density and life cycle, they are still unable to match the higher autonomy and lower cost of modern fuel based vehicles. Adding to that, there are other problems that might affect the large scale adoption of EV: Battery recycling issues and city planning for the required large number of plug-in charging stations. All these concerns brought special attention to the dynamic inductive wireless power transfer technology (I-WPT).

A. Inductive Wireless Energy Transfer

The transfer of electric energy by inductive means is a phenomenon long known, a phenomenon that has been extensively experimented e publicized by Nikola Tesla in the late 19th century. Details of the theory involved have been deeply investigated in the past decades, excellent introductory publications being referred as a review of the theory and some of its applications transport systems ([2], [3], [4]).

In fact, the use of inductive wireless energy transfer as a technique to power moving electric vehicles was early reported by California Partners for Advanced Transit and Highways (PATH) [5]. Other relevant and more recent antecedents on dynamic I-WPT include the KAIST OLEV Bus [6] and the ORNL design [7], which inspired this work.

B. Lightweight Electric Vehicles

The overall energy efficiency of most electric vehicles is, however, still strongly affected by the mass proportion of the EV to its payload or passenger. For many urban transport circumstances, the point is, why having to displace a 1 ton vehicle along with a single passenger that weights less than 100 kg? That could be a design paradigm inherited from the thermal engine vehicles, where the engine itself was usually very heavy, requiring a robust and also heavy chassis to be installed on. The combined use of dynamic I-WPT and e-bikes may help solving this intrinsic efficiency problem, with advantages, considering that the bike, in European urban areas, is often quicker than a car, on distances less than 5 km, incidentally, the maximum distance involved in 50% of all European automobile displacements [9].

In this work, we explore a dynamic I-WPT design and the first experimental results of an inductive lane for e-bikes. Due to the lightweight nature of these vehicles, special care is taken to guarantee that ICNIRP [11] recommended maximum levels of human exposure to magnetic fields are verified during design phase, aiming a successful conformity validation of the prototype in a future implementation phase.

*Research partially supported by grant SFRH/BD/52349/2013 from FCT, the Portuguese funding agency supporting science, technology and innovation, under the scope of the MIT-Portugal Program.

L. A. Lisboa Cardoso and J. L. Afonso are with the Centro ALGORITMI, Department of Industrial Electronics, University of Minho, Campus de Azurém, 4800-058 Guimarães, Portugal (tel. 351-253-510183; e-mails: lisboa.cardoso@ieee.org, jla@dei.uminho.pt).

M. Comesaña Martinez and A. A. Nogueiras Meléndez, are with the Department of Electronics Technology, University of Vigo, Vigo, Pontevedra 36310, Spain (e-mail: aaugusto@uvigo.es).

II. SYSTEM DESIGN

A. Design Directives

Some of the design directives express essential functional requirements, while others emphasize cost reduction measures. Among the first class of directives are (P.1 to P.5):

(P.1) The system should be safe under the electric and electromagnetic point of view, for the cyclists and for the general public. Exposure level to the magnetic field from primary coils of inductive lane should be limited according to the International Commission on Non-Ionizing Radiation Protection (ICNIRP) recommendations.

(P.2) The inductive power of a lane module should remain off where there is no EV authorized to harvest energy from it. This should specially hold when pedestrians or other non electric bikes are traveling on the lane.

(P.3) While no two cyclists or EV are expected to ride side by side, the inductive lane should be capable of handling simultaneous multiple EV, including e-bikes, provided a minimum spacing of between two consecutive vehicles is observed (in the prototype, this guard space is established to be 2 meters).

(P.4) If an e-bike traveling on the lane is stopped over an inductive primary coil or if it drifts away from that coil (laterally, for instance), the lane should sense it and immediately shut off that coil.

(P.5) Maximum speed at which energy transfer from lane to bike is guaranteed is 45 km/h. (In many countries this number could be further restricted down to 25 km/h, the legal maximum speed for electric power assistance in PEDELEC type e-bikes.)

E-bikes and other cycles are usually inexpensive vehicles, if compared to other larger EVs, therefore, an inductive lane for e-bikes is expected to have compatible costs. Previous dynamic inductive designs reference an extensive use of expensive soft magnetic materials such as ferrites [6], to concentrate the magnetic field in between primary and secondary coils, thus creating a larger inductive coupling factor k between them and obtaining more efficiency in the energy transfer. In this design, however, trading efficiency for lower costs per km of lane, the following design paradigms are then also adopted (P.6 to P.8):

(P.6) Avoid the use of ferrites and soft magnetic materials of any kind in the inductive lane primary coils design.

Another standard approach for increasing efficiency that often leads to higher costs is the use of litz wire, in both primary and secondary coils. The litz wire consists of a cable with multiple, parallel, smaller diameter insulated wires, in place of one single larger diameter wire. It is built like this because at high frequencies, practically all the current that flows through a circular cross-section wire concentrates in a thin cylindrical external layer, making it more efficient (less resistivity) to use several thinner wires in parallel than to use just one conductor with the integral cross-section area of all thinner wires. The width of this layer, δ, is called skin depth [12], and it can be calculated by (1):

$$\delta = \sqrt{\frac{\rho}{\pi f \mu}}, \qquad (1)$$

were ρ is the resistivity of the wire, μ its magnetic permeability and f is the frequency of the electric current.

If the diameter of the wires is small compared to δ (calculated for a given frequency), that permits the use of the whole cross-section of each wire, what helps keeping the resistive losses low on the conductor (copper). In this work, trying to reduce cabling costs, the use of cheaper standard multi-conductor cables of suboptimal litz diameters was also explored, constituting another design paradigm:

(P.7) Restrict the choice of cables for the primary coils to commercially available cables of, if necessary, suboptimal litz diameter, sacrificing system electrical efficiency for a reduction in the lane cost per km.

(P.8) Minimize the need for coding new software. Any communication between lane and vehicle should be preferentially based on existing standard protocols.

B. Inductive Lane Architecture

The system comprises two main parts, the inductive lane itself and the vehicle (e-bike). The inductive lane is formed by a sequence of oblong primary coils modules embedded underneath ground level, along the vehicle path, that can be independently excited by high frequency alternating current. The oscillating magnetic field of each primary coil is then individually enabled when a Radio Frequency Identification (RFID) tag on board of the e-bike is detected and authenticated by an auxiliary coil on the lane, laying closely to that primary coil. Beyond transponding the vehicle identification code, the tag also contains a parameter that defines the maximum power level the vehicle might demand, allowing the lane to adjust the inverter output accordingly.

Vehicles of dissimilar power demands can therefore be simultaneously served on the lane, by coupling to the lane though its different primary coil modules. Since the length of a single primary coil is barely enough to receive a single e-bike, there is no need to manage multiple bikes on the same inductive module.

Aiming a simplified installation of the inductive lane in public space, coils are paired as shown in Fig. 1 and Fig. 4, such that all electronics for two neighbor coils can physically reside in a single junction box, thus dividing by two the number of boxes per kilometer. The LF inverter, shown in the same Fig.1, is actually a pair of synchronous inverters, controlled by one single PWM (pulse width modulation) block (Fig. 2). In this first design phase, oscillating frequency was set 51.7 kHz, high enough to experimentally attain electric efficiencies greater than 50% over the 13.5 cm design air gap between primary and secondary coils, and low enough to permit the use of inexpensive, widely commercially available copper cables with 1 mm^2 and 1.5 mm^2 of cross sectional area, with no excessive skin effect losses. In fact, at 51.7 kHz, the skin depth is approximately 0.28 mm^2, resulting in the effective use of roughly 75% of a 1 mm^2 copper conductor.

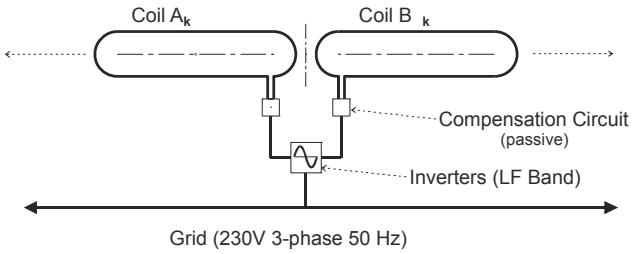

Figure 1. Dual-coil dual-inverter inductive lane power module.

Each of the inverters is coupled to a primary coil though a compensation circuit that is closely tuned to the oscillating frequency, resulting in a low total harmonic distortion on the currents passing through the primary coils. Also, due to the resonant tank formed by the parallel association of primary coils and the compensation capacitor, those currents are much higher than the currents supplied by the inverters, which generate losses on the MOS FETs (power transistors).

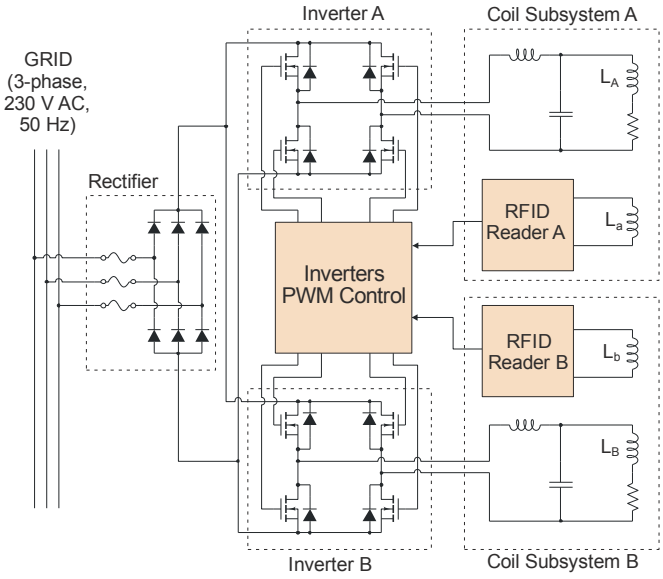

Figure 2. Diagram of the induction power transmitter, on the lane side.

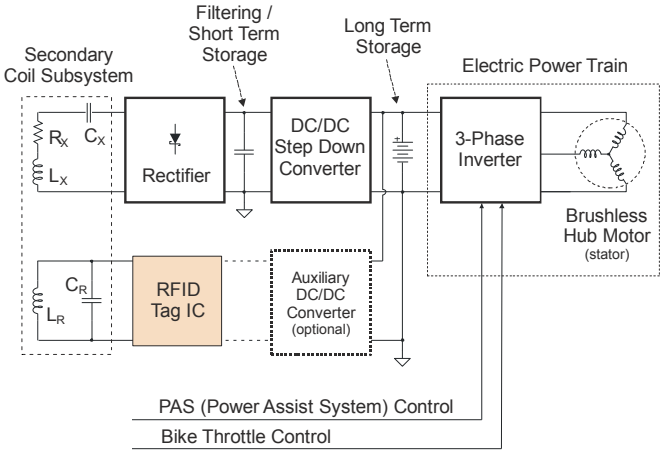

Figure 3. Diagram of the induction power receiver, on board of the e-bike.

Depending on the proportion of inductive lanes in a route design, and on particular vehicle applications, it is possible for the e-bike to either require less charging stops or even to completely dismiss the use of standard batteries, relying solely on on-board super capacitors for short-term energy storage, as shown in Fig. 3, while tracking the inductive lane, or on pedaling, while away from it.

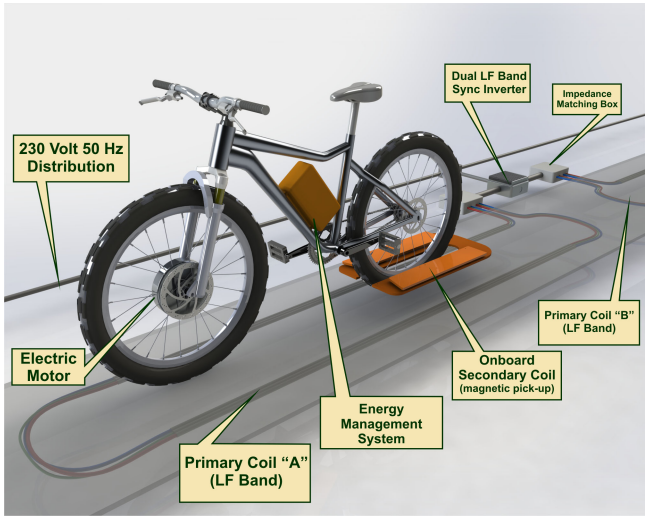

Figure 4. Adapted e-bike with pick-up coil and energy management system, represented on the inductive lane in normal riding position.

C. *RFID for Intelligent Lane Power Control*

Beyond conveying vehicle authentication information, the on-board RFID tag explicitly informs the primary inductive module, which the EV is driving power from, about the power level currently demanded, thus permitting each primary coil to be energized at the minimum required power level, reducing energy losses and resulting in a system with improved overall energetic efficiency. Because of this explicit power demand, it is also possible for the lane to efficiently handle vehicles with dissimilar power requirements, provided the power demand is limited to a maximum design level.

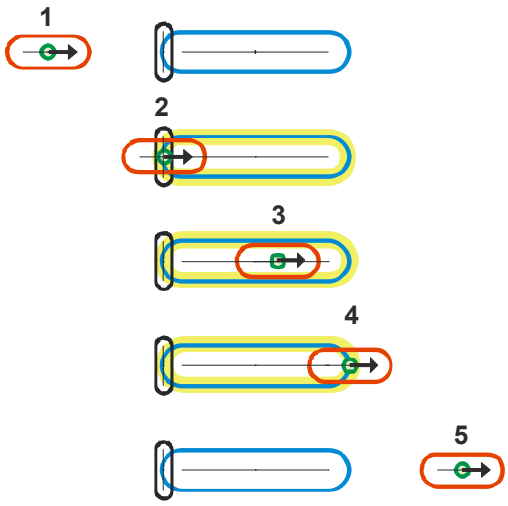

Figure 5. Sequence of events ilustrating one possible design interaction of the RFID subsistem to control the power of a primary coil (top view).

One of the simplest strategies for using a RFID for enabling the power a primary coil, the gated control, is illustrated in Fig. 5: mounted on board of the EV, which is coming from left (position 1), are a power pick-up coil (red) and a RFID tag with its coil (green). When the vehicle RFID tag is detected by the RFID reader coil (black) laying in the left extremity (the "gate", position 2) of the primary coil (blue), the primary coil is energized (yellow halo) and power transfer is initiated. Power is sustained while the EV is over the primary coil and continuously demands it (position 3), regardless of RFID reading status. When the pick-up coil crosses a point of zero coupling (position 4) and the power demand momentarily decays bellow a control limit, the inverter feeding the primary coil is then shut off, until the next RFID activation, while the EV continues its journey to the next primary coil. If power demand is stopped when the EV is still over a primary coil, what may happen, for instance, if the EV's electric motor is cut and battery is not being recharged, or if the cyclist stops, the lane immediately senses it and shuts off the primary coil as well.

In the gated control strategy, because RFID detection and authentication are required at the approach of primary coils, RFID reader coils must be installed on both ends for the lane to work bidirectionally. In this basic strategy, a problem could result if a second non-authorized vehicle would come closely after the first, in the same wrong way – condition when the system could possibly be defrauded, supplying energy for the second non-authorized vehicle after reading the authorization code of the first EV. But the discussion of these issues is out of the scope of this first conceptual design.

III. CONTROL OF MAGNETIC FIELD EXPOSURE

When electric devices are supposed to be used in close contact with human beings, one of the main concerns is to limit field exposure, in order to avoid biohazards. In 1998, the International Commission on Non-Ionizing Radiation Protection (ICNIRP) published, based on existing previous studies, guidelines for limiting human exposure to time-varying electric, magnetic, and electromagnetic fields, a document that was partially updated in 2010 [11] and is widely adopted by designers and manufacturers. According to these guidelines, in the frequency band from 3 kHz to 10 MHz, the recommendable maximum magnetic field intensity for general public and occupational exposures are 27 μT and 100 μT (rms values), respectively, provided the dimensions of the structures generating the magnetic field are such that electromagnetic irradiation can be neglected at the given frequency of operation.

In our system, the ICNIRP design compliance was initially accomplished by finite element magnetic field simulation, using the FEMM 4.2 software which is free public licensed tool [8]. Using the actual current values injected in the primary coil, a simulation was conducted, resulting in the magnetic field which cross section is drawn in Fig. 6, superimposed to the bike (to scale). It can be easily seen that, in normal riding position, the whole cyclist body, except ankles and feet, would be in a region of the space where general public expose reference levels (≤ 27 μT rms value) are observed. Still, the exposition of these lower body parts to magnetic fields would lay within the occupational exposure reference level limit of 100 μT rms value. The present verification is considered only as preliminary, because the FEMM tool used restricts the numeric solution to have planar symmetry, not being capable to perfectly model this richer 3-dimensional problem. Also, the tests of prototype so far did not include the actual measurement of magnetic field values. These are essential tasks yet to be done in the next phases of the development.

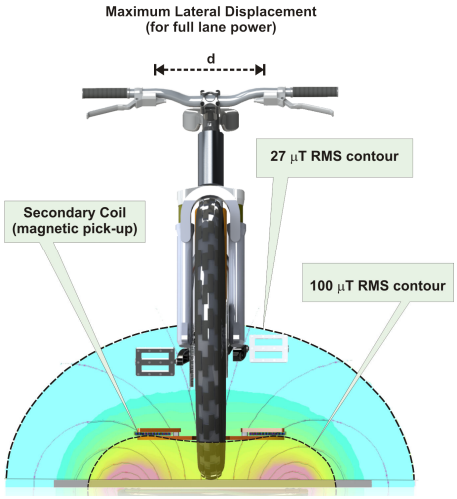

Figure 6. Front view of e-bike adapted with pick-up coil, represented on the inductive lane when its magnetic field is turned on.

IV. EXPERIMENTAL RESULTS

The bike used to build the prototype was a standard, non-electric, 29-inch wheel bicycle, with aluminum rims and frame. Avoiding the use of ferromagnetic materials in the assembly is very important, not introduce power losses by means of hysteresis. The choice for the wheel size, on the other hand, was due to the fact that this size generally leads to better clearance from pedals to ground, and the same time provides more room for a larger secondary coil to be installed around the (rear) wheel. The first step in the prototype setup was then to convert this bike to electric, minimally by installing an electric motor, an inverter and the throttle control, that is connected to a sensor input of the inverter, to vary the speed of the bike. The bike-coil assembly was tested neither to exhibit mechanical interference between pick-up coil and pedals nor between pick-up coil and flat ground, even when ridding in sharp turns and moderate speeds.

E-bikes today usually have the electric motor installed either in the front or rear wheel, or in a central position ("mid-drive"), case in which the bike frame is often specifically designed for electrification. We opted to install it in the front, for the ease of having separated installations for the motor (front wheel) and the pick-up coil (rear wheel). Its nominal power was chosen at 300W, so that it could handle 250W with safety margins, the nominal maximum power of most PEDELEC type cycles (400W peak, for short periods).. A small 7Ah 36V battery was also installed, just to allow functional tests of the bike as a standard electric vehicle. The other electronic subsystems, a full wave bridge rectifier with Schottky diodes and a programmable DC-to-DC step down converter, that stabilizes the voltage (36V) for the motor inverter, were mechanically integrated in the frame of the bike, together with a DC power meter (Fig. 7).

Figure 7. E-bike specially adapted with a pick-up coil and power circuitry, shown during workbench tests.

The tests for power transmission were performed with the bike and lane assembled on workbench (Fig. 8). For simplicity, bike was run in electric only mode (no pedaling). This first prototype consisting of a lane segment with just one 3.25 m long primary coil, delivers 400 W of power to an e-bike over its whole length, with an acceptable lateral bike to lane misalignment diameter of up to roughly 20 cm. This width climbs to 29 cm at 200 W (-3 dB). The lane is also able to supply 250 W (the value of maximum nominal power recommended for standard power assisted electric cycles - PEDELEC), within ±13.5 cm (27 cm width) of lateral misalignment. These results are shown in Fig. 9 and Fig. 10 and summarized in Table I.

TABLE I. MAXIMUM LATERAL MISALIGNMENT WIDTH

Power (W)	EV to Lane Maximum Misalignment Width (cm)
400 (PEDELEC* peak)	20
250 (PEDELEC* max)	27
200 (-3 dB point)	29

*Pedal assisted electric cycle.

The power sensitivity to roll angle was not actually measured in these first experiments; however, the power delivered to load was noticed to have just a small variation when the bike was inclined representative ridding angles left or right, with the bike standing on a central position in lane.

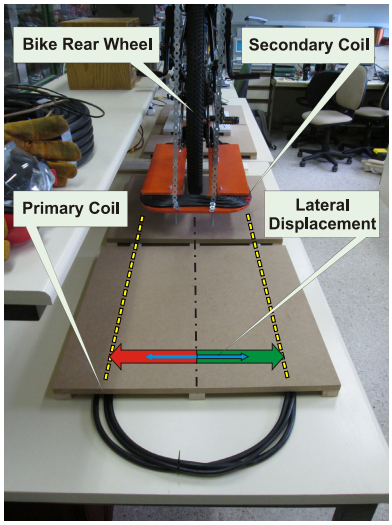

Figure 8. Rear view of the prototype assembly, with the adapted e-bike mounted on the inductive lane, for workbench tests.

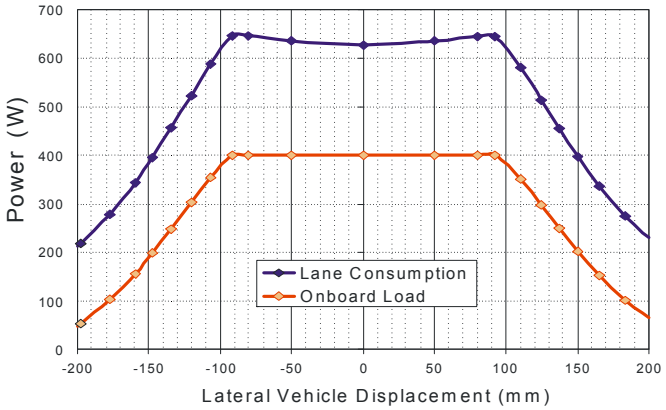

Figure 9. Power demand of lane inverter (blue) and net power on load (red) as a function of lateral bike misalignment to lane.

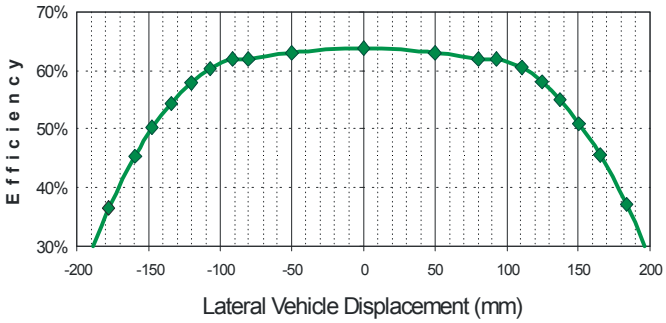

Figure 10. Measured electrical efficiency of the developed prototype.

In the experimental validation of the RFID technology for power control, ISO/IEC 14443A RFID reader and tag (13.56 MHz) were tested. In order to extend identification range, the RFID magnetic antennas were resized, the reader coil to 29 x 50 cm, single loop, and the tag coil to 13 cm of diameter, six turns, to make them compatible with the lane dimensions and the gated control strategy shown in Fig. 5. In initial tests, using the redesigned RFID coil antennas, successful authentication were achieved with reading cycles of less than 32 ms in a volume of 27 cm x 25 cm x 23 cm (width x length x height). That reading distance exceeds the 13.5 cm design gap existing between primary and secondary power coils, making it possible to install the tag on the pick-up coil and use this RFID technology to provide EV authentication for the lane. This permits at least one successful RFID detection during the RFID tag transit over the tag reader, gating the inverter, provided the vehicle's maximum speed is limited to 25 cm / 32 ms, roughly 28 km/h. That speed is higher than the 25 km / h maximum speed usually adopted for limiting power assistance in PEDELEC bikes. The 25 cm maximum undetected trajectory of the vehicle is small when compared to the primary coil length (3.25m), what means that there will be no significant reduction (7.7% worst case – ~4% average) in the power transfer duty cycle, as a consequence of the vehicle speed.

Although the newly designed coils are not part of the RFID ISO standard, no modification was done to the protocol, reducing the development effort for the control software. At the current stage of the work, however, the RFID reader and lane inverter are not yet integrated, a task to be completed in future experiments.

V. CONCLUSION AND FUTURE WORK

An inductive lane and the adaptation of an e-bike to use it were designed, prototyped and tested. The built prototype consists of a first 3.25 m lane segment with just one primary coil, capable of delivering 400 W of power to an e-bike over its whole length, with an acceptable lateral bike to lane misalignment diameter of roughly 20 cm. The lane is also able to supply maximum nominal power (250 W) for standard power assisted electric cycles (PEDELEC) within 27 cm of lateral misalignment. While current lane prototype does not fully implement all details of the proposed design, the results so far obtained are representative of the power levels involved, preliminarily demonstrating the feasibility of this new modal variant for urban lightweight transport.

The design paradigms adopted yielded a system that is predicted to have a potentially low cost to implement, compatible with the cost of the vehicles it is intended to be used with, at the expense of a degraded electric efficiency. Detailed cost estimates have not yet been evaluated though. While the 64% peak DC-to-DC efficiency measured on the prototype is significantly lower than those reported in recent achievements in dynamic inductive wireless power transfer, the intrinsically lower power consumption of lightweight vehicles, associated with the predicted low cost of the system, can still make it possible to consider its advantageous use in urban environment. This opens new possibilities for the sustainable use of e-bikes and similar electric vehicles for personal mobility, such as electric wheel chairs, tricycles and rickshaws. Additionally, the system efficiency is expected to be improved in future implementations of the system, by the increase of the induction frequency and the use of more advanced power electronics blocks.

In this manner, many opportunities for further research and system improvement are foreseen:

- Explore the use of higher induction frequencies, particularly, determining whether the new SAE Std TIR J2954 [10] could be advantageously applied in this dynamic application as well. (The inductive frequency band this standard recommends for compatibility of newer stationary automotive I-WPT design goes from 81.39 kHz to 90 kHz.)
- Perform more precise magnetic field simulations with 3D finite element modeling tools, and actually measure it, to guarantee full ICNIRP-2010 compliance. If necessary, redesign bike components and pick up coil arrangement, in order to achieve it.
- Analyze the possible insertion of soft magnetic materials (on board of bike only), in the coil pick-up design, seeking to improve system efficiency without increasing the per km cost of the lane implementation.
- Improve the efficiency of system power electronics, by adopting modern circuit variants for the inverters and rectifiers, both on lane and on vehicle.
- Adopt additional design techniques to improve quality of power demand and minimize eventual impact on grid.
- Optimize the design considering the bike dynamics, to improve bike maneuvering flexibility on lane.
- Propose urbanistic and engineering solutions integrating inductive lanes with existing bike lanes and other public transport infrastructures.
- Analyze the combined use of grid and off-grid renewable energy (solar and wind), to extend the use of this inductive lane design for neighborhood and interurban service.
- Analyze the social, environmental, economic and legal aspects of mixing public inductive infrastructure and private lightweight vehicles.

ACKNOWLEDGMENT

The authors are grateful to the support received from the Portuguese Agency for Science and Technology (FCT) and the *b*ike drawings provid*e*d by Mr. Ricardo Pérez Rodríguez, which were modified to ob*t*ain some of the figures. Mr. L. Cardoso also thanks the guidance on ind*u*ctive wireless power tran*s*fer technology received from prof. Stanimir Stoyanov Valtchev, from Universidade Nova de Lisboa.

REFERENCES

[1] Electric Vehicles, 2008. In "The Gale Encyclopedia of Science", 4th Edition, K. L. Lerner and B. W. Lerner, editors. Detroit: Gale Cengage Learning, Vol. 2, pp. 1474-1477.

[2] G. A. Covic and J. T. Boys, "Modern Trends in Inductive Power Transfer for Transportation Applications," in IEEE Journal of Emerging and Selected Topics in Power Electronics, vol. 1, no. 1, pp. 28-41, March 2013.

[3] G. A. Covic and J. T. Boys, "Inductive power transfer," Proc. IEEE, vol. 101, no. 6, pp. 1–14, Jun. 2013.

[4] S. Li and C. Mi, "Wireless power transfer for electric vehicle applications," IEEE J. Emerg. Sel. Topics Power Electron. , vol. 3, no. 1, pp. 4–17, Mar. 2015.

[5] Systems Control Technology Inc., "Roadway powered electric vehicle project: Track construction and testing program phase 3D," California PATH Program, Inst. Transportation Studies, University of California, Berkeley, CA, USA, Tech. Rep. UCB-ITS-PRR-94-07, 1994.

[6] S. Lee et al, "On-Line Electric Vehicle using inductive power transfer system," 2010 IEEE Energy Conversion Congress and Expositon, Atlanta, GA, 2010, pp. 1598-1601.

[7] J. M. Miller et al., "Demonstrating Dynamic Wireless Charging of an EV: The Benefit of Electrochemical Capacitor Smoothing," in IEEE Power Elec. Mag., vol. 1, no. 1, pp. 12-24, March 2014.

[8] D. C. Meeker, Finite Element Method Magnetics, Version 4.2 (12 Jan 2016 Build), http://www.femm.info

[9] European Cyclists' Federation. "Future cities are cycling cities!", March, 2009. http://ec.europa.eu/transport/themes/strategies/consultations/doc/2009_03_27_future_of_transport/20090326_ecf.pdf

[10] Society of Automobile Engineers (SAE), "Wireless Power Transfer for Light-Duty Plug-In/ Electric Vehicles and Alignment Methodology," SAE Technical Information Report (TIR) J2954, May, 2016.

[11] ICNIRP, "Guidelines for limiting exposure to time-varying electric and magnetic fields (1 Hz to 100 kHz)", Health Phys., 99(6), December 2010, pp. 818-836.

[12] J. D. Jackson, Classical Electrodynamics, 3rd ed. New York: John Wiley and Sons (WIE), 1998, chapter 5, sect. 5.18, pp. 219-221.